International Journal of Multidisciplinary Research and Development

IJMRD 2014; 1(7): 407-410
www.allsubjectjournal.com
Received: 10-12-2014
Accepted: 26-12-2014
e-ISSN: 2349-4182
p-ISSN: 2349-5979

Chirag Gupta
Department of ECE, ITM University

Divyanshu Singh
Department of ECE, ITM University

Nitin Garg
Department of ECE, ITM University

Correspondence:
Chirag Gupta
Department of ECE, ITM University

Measurement and implementation of antenna radiation pattern

Chirag Gupta, Divyanshu Singh, Nitin Garg

Abstract
In a recent paper, a nascent technique that allows to perform actual antenna radiation pattern measurements in reverberation chamber (RC) has been presented and then the radiation pattern are used to form 3D radiation pattern of the horn antenna. In this contribution, an improvement of this technique is presented; an antenna radiation pattern is obtained by performing only one measurement per angle under study, taking advantage of real-time Doppler Effect. In order to display the validity of this improved technique, the radiation pattern for both E- and H- planes of a horn antenna is measured in an RC, the results obtained in are matching with the result obtained in AC and the values provided by the antenna manufacturer, respectively. Furthermore, these radiation patterns are used with various approximations to demonstrate the antenna radiation pattern in 3D using MATLAB.

Keywords: Antenna measurements, antenna radiation patterns, electromagnetic radiation, microwave measurements, reverberation chamber, H-plane radiation pattern, E-plane radiation pattern.

1. Introduction
Today, due to a rapid progress in mobile communication demands to a necessity of propagation planning and modelling. Providing adequate good service, which is consider as good signal coverage and minimum interference, it requires very precise description of propagation environment. More precise the description is the better results are found in general. So it can be inferred that the accurate knowledge of an antenna's radiation pattern can leads to better results of the propagation prediction.

Reverberation chambers (RCs) is proposed to 3GPP in Technical Report 37.976 [1] as one of the candidate methodologies for testing of multiple-input-multiple-output (MIMO) over-the-air (OTA) performance, and its standardization is underway [2].Nevertheless, the same Technical Report which is based on contemporaneously available information, postulates that antenna radiation patterns can't be measured, if needed, with this candidate methodology based on RC [1].

However, a time-reversal electromagnetic chamber was purposed to regain the free-space radiation pattern of an antenna under test (AUT), but the proposed procedure has only been supported by a two-dimensional numerical simulation [3]. A new technique that allowed for the first time to perform actual measurements of antenna radiation pattern in RC has been presented in a recent paper [8]. Plane wave decomposition and a spatial Doppler analysis are used in this technique, moving the AUT in order for obtaining the Doppler power spectral density, and eventually, the AUT radiation pattern. Although, the results provided by this technique were matching with the ones obtained in anechoic chamber (AC), it was essential to analyse measurements with the transmitting AUT which was located at N different points with its line-of-sight (LOS) to a fixed receiving antenna.

On the other hand, in this paper, an improvement to this technique is being explained, obtaining an antenna radiation pattern by performing only one measurement per angle under study, taking advantage of real-time Doppler Effect, thus being faster than in [8], and being obtained in a similar accuracy. In order to support the validity of this technique, the radiation pattern for both E- and H- planes of an X band horn antenna has been measured in an RC at 10 GHz (X band centre frequency), and compared with the ones obtained in AC, result obtained were satisfactory. Furthermore these result were plotted in 3D after various approximations using MATLAB.

2. Radiation Pattern Measurement Methodology

Let us consider any signal generator connected to a fixed antenna which emits a continuous wave (CW) signal at certain frequency f_c, and a receiver AUT, both these antennas are in LOS inside an RC. Also define the AUT initial orientation (θ_o,φ_o), these initial orientation is in spherical coordinates. When the emitter antenna is fixed and the receiver AUT is being rotated through angles ($\Delta\theta$,$\Delta\varphi$) relative to its initial orientation, the transmitted power LOS component is in straight variation to the AUT radiation pattern $G(\theta,\varphi)$, with $\theta=\theta_o - \Delta\theta$, $\varphi=\varphi_o\Delta\varphi$. Thus, in order to calculate this AUT radiation pattern $G(\theta,\varphi)$, it is necessary to differentiate this LOS component from all other non-line-of-sight (NLOS) multipath components [8]. For this, the receiving AUT has been employed to a linear rail orientated along the LOS to the fixed emitter antenna, and moved toward it with a constant speed υ. As a result, the AUT will receive the component of LOS at a frequency $f_r = f_c+f_d$, where $f_d = f_c\upsilon/c$ is the maximum Doppler frequency shift ξ from the centre frequency f_c which can be obtained due to the velocity υ ,where c is the speed of light. As the Doppler frequency shift depends on its angle-of-arrival (AoA) comparable to the LOS such that $\xi = f_c\upsilon\cos(\alpha)/c$, max Doppler frequency shift will only be observed when the AoA is aligned with the LOS, which is, $\alpha=0$, which is only the case of the LOS component, as depicted in Fig. 1. However, to distinguish this LOS component coming from the direct path at the frequency $f_c + f_d$, from the reflected NLOS component received from the opposite direction at the frequency $f_c - f_d$, an I/Q demodulator has been inserted, using as radio frequency signal (RF) the received one at frequencies $f_r = f_c + \xi$, where $-f_d < \xi < f_d$, and as local oscillator signal (LO) the same continuous wave at the Frequency f_c as the emitted one, thus a demodulated signal that is time-domain Doppler signal at frequencies ξ is obtained, being the LOS component arriving from the direct path at a frequency.

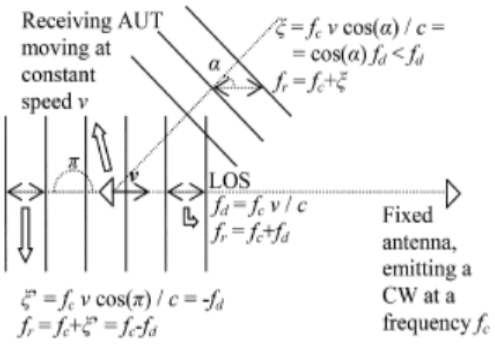

Fig. 1. Different Doppler frequencies for different AoAs.

$\xi = f_d$ and the reflected NLOS component which is received from the opposite direction at $\xi = - f_d$, make result easy to be discriminated. Therefore, because a CW at a frequency f_c emitted by fixed antenna, and being the receiving AUT rotated through angles ($\Delta\theta$,$\Delta\varphi$), we can calculate Doppler power spectral density $D(\xi)$ as the squared absolute value of the Fourier transform $X(\xi)$ of the time-domain complex signal foe which real and imaginary parts are the in-phase and quadrature components of the demodulated received signal I(t) and Q(t) as described in equation 1, where F(…) is the Fourier transform with respect to time t. Thus $D(\xi)$ can be obtained from only one real-time measurement in time domain without any additional stirring. As it will include, among others, the desired LOS component at the maximum Doppler frequency shift f_d, the desired AUT radiation pattern $G(\theta,\varphi)$ at a frequency f_c can be obtained as equation (2).

$$D(\xi) = D(f,\xi,\theta,\varphi)\Big|_{f=f_c,\theta=\theta_0-\Delta\theta,\varphi=\varphi_0-\Delta\varphi} = \left|\mathcal{F}\{I(t)+jQ(t)\}\right|^2 = \left|X(\xi)\right|^2 \quad (1)$$

$$G(\theta,\varphi) = G(f,\theta,\varphi)\Big|_{f=f_c} = D(\xi)\Big|_{\xi=f_d} = D(f_d). \quad (2)$$

As the reflected NLOS component received from the direction opposite to the LOS will be contained in $D(\xi)$ at the negative Doppler frequency shift - f_d, it will be discriminated easily. On the contrary, a demodulation based on a mixer retrieving only the in-phase component of the received signal I(t), would have averaged both and I(t) and Q(t) at the Doppler frequency shift of interest f_d, causing the consequent error introduction in inverse variation to the AUT front-to-back ratio at its orientation (θ,φ), that is, $G(\theta,\varphi)/G(\Pi - \theta,\varphi + \Pi)$.

3. Polynomial Approximation

3.1. Simple polynomial interpolation

It is never used for smoothly approximate large number of values. In this approximating curve is oscillating through the values.

4. Trigonometrically polynomial interpolation

It is mostly useful for approximation of periodical functions. For approximating large number of measured values is not suitable in this interpolation.

5. Chebyshev approximation

It is very precise and accurate but too complicated method for processing of large number of measured values of antenna diagrams.

6. Spline functions

The bilinear interpolation by cubic spline function is found most suitable due to, this method is capable to fulfil all criteria mentioned above. The result surface in this is quite smooth because splines join continuous low order (three for cubic spline) polynomials which satisfy smoothness assumption. In this method the approximation error is much smaller than error of other methods and it can be used for approximation of all types of antennas diagrams. Using B-splines (Coons's cubics) ensures relatively low demand on computer time consumption.

7. Interpolation by Rational Functions

It can be also used for this approximation, especially for interpolating values from catalogue or estimated from the expressions of The Vienna agreement. Problems start when interpolating of measured values is needed. Interpolating curves or planes are trying to go through all values presumably influenced by errors of measurement and therefore the error of the approximation is increasing. It is the main difference from the spline functions that extrapolate measured values to obtain smooth curve.

8. Radiation Pattern Measurement Results

Here f_c is taken as 10 GHz distance L is taken as 1.59 m, which corresponds to 53 λ (wavelength) at 10 GHz approximately. N = 416 samples of I(t) and Q(t) have been recorded in AUT movement (of 13 s). The resulting radiation patterns for both E- and H- planes are depicted in Figs. 3 and 4, respectively, and compared with the ones obtained in AC.

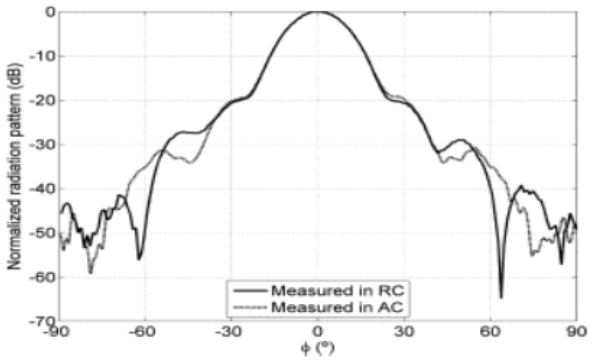

Fig. 2

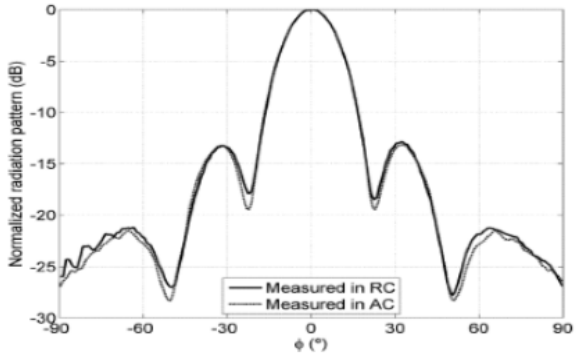

Fig. 3

In order to test the selected approximation method and to specify its error, calculated radiation pattern was compared with measured values and with the approximation made only from its two basic cuts. The flat horn antenna is chosen due to its different vertical and horizontal cuts in the radiation pattern. Thus it's one of the most difficult patterns for the approximation. In the first cut there is only the main lobe without any side lobes, on the other hand, the orthogonal cut has two eminent side lobes. Radiation pattern must be measured at least in twelve spatial cuts to obtain relatively precise 3D pattern by approximation these cuts (Fig. 4)

The bilinear (two-dimensional) interpolation by the cubic spline functions was made only from measured cuts of the radiation pattern of the flat horn antenna and the 3D diagram can be seen in Fig. 5**.**

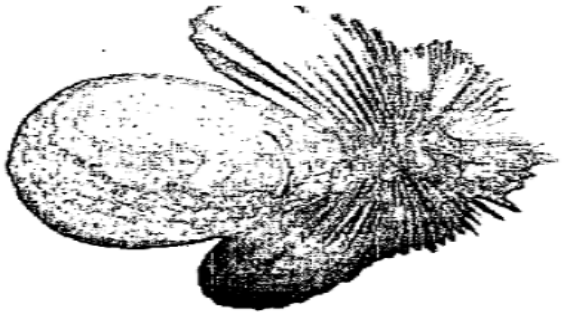

Fig. 4

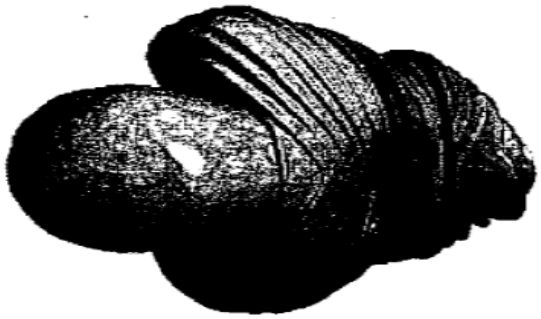

Fig. 5

The maximal difference between the real 3D radiation pattern (approximation made of 11 spatial cuts) and the 3D radiation pattern made only of its two orthogonal cuts is evidently in the area of side lobes in the spatial cut which is exactly between known vertical and horizontal cuts. For comparison of real and approximated spatial cut for the azimuth *q* = 46" (the cut with maximum error) see Fig. 6

The maximum error of approximation is about 12.05db**.** It is very high but the error of all points in other spatial cuts is much smaller. For example the error of approximation for the azimuth (o= 14" is in Fig. 7). The radiation pattern of the flat horn antenna is one of the most difficult diagrams for the approximation because of two different orthogonal cuts. The error of approximation of antennas whose two orthogonal cuts are not so different (with more axially symmetrical diagram) is much smaller as well. The error obtained in axially symmetrical diagram is negligible.

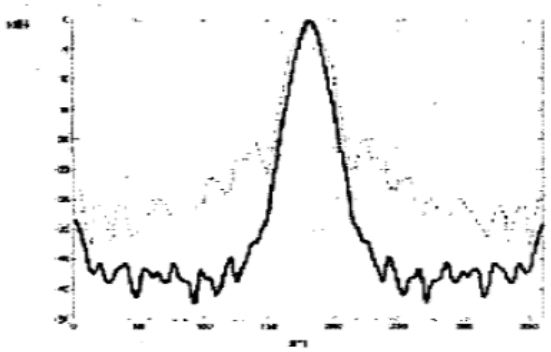

Fig. 6

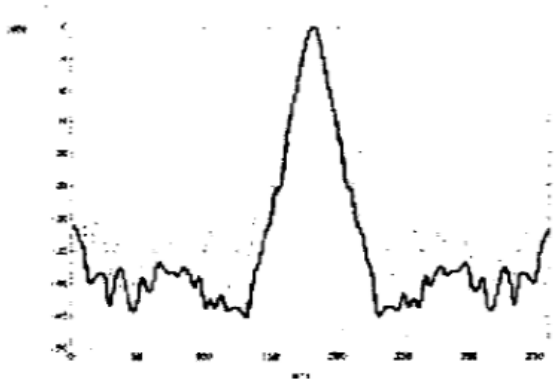

Fig. 7

9. Matlab Implementation

The implementation of the 3D approximation of antenna radiation patterns was implemented in the 'MATLAB environment, which is suitable for calculating with matrices of large dimensions. The angle resolution in the radiation pattern measurement is usually one degree or less.
Measured values are processed in the 3 steps

1) Loading horizontal and vertical cuts of the antenna diagram.
2) Spline functions are used smoothed the error values. These measurement errors are mainly caused by background noise, reflections or angle inaccuracy while taking the values.
3) At last cubic spline is used for the bilinear approximation.

The result of these approximation are depicted in 2 ways as shown in fig. 8 and fig 9.

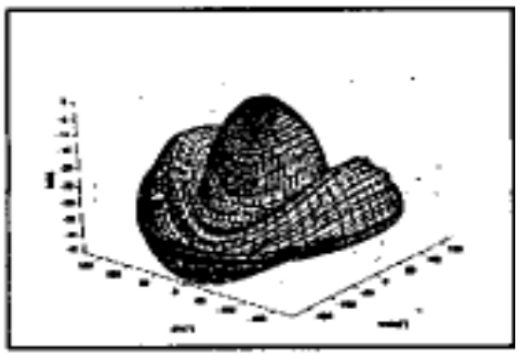

Fig. 8

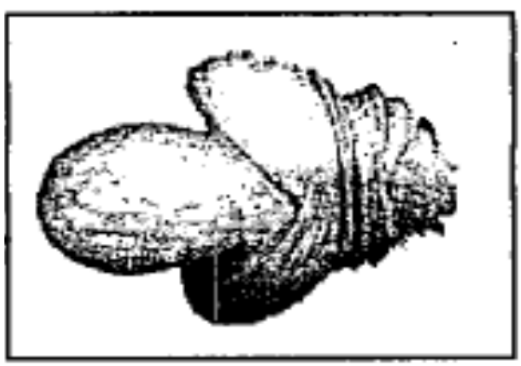

Fig. 9

11. Conclusion

An improvement of the novel methodology presented in [8], used to perform actual antenna radiation pattern measurements in RC for the first time, has been presented and the radiation pattern obtained from this technique is used to draw a radiation pattern of horn antenna in using MATLAB.

12. References

1. 3rd generation partnership project, measurement of radiated performance for multiple input multiple output (MIMO) and multi antenna reception for high speed packet access (HSPA) and LTE terminals (Release 11) 2012, 3GPP Tech. Rep. 37.976 v11.0.0.
2. García-Fernández MÁ, Sánchez-Heredia JD, Martínez-González AM, Sánchez-Hernández DA, Valenzuela Valdés JF. "Advances in mode-stirred reverberation chambers for wireless communication performance evaluation," *IEEE Commun. Mag.*, Jul. 2011; 49, no. 7, 140-147.
3. Cozza A, Abou-El-Aileh A. "Accurate radiation-pattern measurements in a time-reversal electromagnetic chamber," *IEEE Antennas Propag. Mag.*, Apr. 2010; 52: no. 2, 186-193.
4. Lemoine C, Amador E, Besnier P, Sol J, Floc'h JM, Laisné A. "Statistical estimation of antenna gain from measurements carried out in a mode-stirred reverberation chamber," in *Proc. XXXth URSI General Assembly and Scientific Symp.*, 2011, 1-4.
5. Lemoine C, Amador E, Besnier P, Floc'h JM, Laisné A. "Antenna directivity measurement in reverberation chamber from Rician-factor estimation," *IEEE Trans. Antennas Propag.*, Oct. 2013; 61: no. 10, 5307-5310.
6. Lemoine C, Amador E, Besnier P, "On the -factor estimation for Rician channel simulated in reverberation chamber," *IEEE Trans.Antennas Propag.*, Mar. 2011; 59: no. 3, 1003-1012.
7. Fiumara V, Fusco A, Matta V, Pinto IM, "Free-space antenna field-pattern retrieval in reverberation environments," *IEEE Antennas Wireless Propag. Lett.*, 2011; 4:329-332.
8. García-Fernández MA, Carsenat D, Decroze C. "Antenna radiation pattern measurements in reverberation chamber using plane wave decomposition," *IEEE Trans. Antennas Propag.*, Oct. 2013; 61: no. 10, 5000-5007.
9. Shannon CE. "Communication in the presence of noise," *Proc. IRE*, 1949; 37: no. 1, 10-21.
10. Friis HT. "A note on a simple transmission formula," *Proc. IRE*, May 1946; 34, no. 5, 254-256.
11. Coding instruction for antenna diagrams, Vienna agreement, 1999, Annex 6
12. Allard RI, Werner DH. The Simulteneous Interpolation of Antenna Radiation Patterns, IEEE Transaction on Antennas and ProDaeation. @, March 2000, 383-391.
13. Gil F, Claro AR, Pardelinha C, Correia LM. IEEE Antennas and ProDacation Maeazine, fi April 2001, 132-137.